Effect of polymer coating on the magnetic properties of oxygen-stabilized nickel nanoparticles

Vidyadhar Singh and V. Srinivas*
Department of Physics and Meteorology, Indian Institute of Technology, Kharagpur 721302, India

M. Ranot, S. Angappane,† and Je-Geun Park‡
BK21 Division, Department of Physics and Department of Energy Science, Sungkyunkwan University, Suwon 440-746, Korea
(Received 9 September 2009; revised manuscript received 22 July 2010; published 12 August 2010)

A comparative study of the structural and magnetic properties of polymer coated (pc-) and uncoated (uc-)Ni nanoparticles prepared by chemical reduction method are reported. pc-Ni nanoparticles have been synthesized by reducing Ni^{2+} cations to Ni particles by sodium borohydride in aqueous solution in the presence of polyvinyl alcohol (PVA) solution. Both samples have been identified to have a tetragonal crystal structure, different from its usual fcc structure, though some traces of fcc-Ni phase have been observed in x-ray diffraction and selected area electron diffractogram patterns for pc-Ni. This structural modification of fcc-Ni occurs due to the presence of interstitial oxygen atoms in the Ni lattice and results in appreciably modified magnetic properties in this new phase of Ni, as, for example, a nonhysteretic magnetization response with applied field at 300 K. A comparative magnetic study of the uc- and pc-Ni particles exemplifies the role played by the PVA matrix in modifying the magnetic properties of the uc-Ni sample. The *M-H* and *M-T* curves have been analyzed using superparamagnetic/ferromagnetic/paramagnetic component models and anomalies observed were explained using two-phase model.

DOI: 10.1103/PhysRevB.82.054417 PACS number(s): 75.75.−c, 75.40.Gb, 75.30.Kz, 75.25.−j

I. INTRODUCTION

The synthesis of nanoscale materials with desired properties is rather tricky and presents a great challenge to the scientific community. The frequently encountered obstacle during the synthesis of metal nanoparticles (NPs) is the spontaneous production of oxides due to very high surface-to-volume ratio of the particles. As a result metal NPs are being encapsulated within a spontaneous surface oxide (SSO) layer, form in what is known as a "core-shell" structure.[1–3] NPs having the core-shell morphology are of interest in their own right and have been the subject of extensive research in the recent past.[4–10] For example, in many solar absorbing coatings, the presence of a dielectric/insulating shell around at least part of the metallic core severely delays the oxidation and appears to be the main reason for their high stability. However, one of the major disadvantages is that the oxide coating close to the transition metallic core (e.g., Fe, Co, and Ni) induces weakening in the exchange interactions of the surface atoms with the surrounding ones thereby modifying the magnetism and other related properties to an appreciable extent.[11] Apart from the oxide layer, the magnetization of nanocrystalline ferromagnets (FMs) are also reported to be highly sensitive to oxygen contamination. A rough estimate shows that every oxygen atom destroys the contribution of one Ni atom to ferromagnetism and leads to a strong decrease in magnetization.[12] The SSO layer and absorbed oxygen in magnetic NPs thus itself merit an in-depth study. Apart from this the surface disorder can also provide material with broken bonds, the missing structural periodicity, and the presence of competing magnetic interactions at the surface[13] spin canting and spin-glasslike behavior in the disordered SSO layer and subsequent reduction in the net magnetization of the NPs. Therefore, it is important to develop novel synthesis and stabilization techniques to seize the complete advantage of these novel magnetic nanostructures protected from the environmental degradation.[3] One of the ways to evade the formation of SSO layer is to synthesize and encapsulate the NPs with inert, nonmagnetic passivation layers of insulators (Al_2O_3 and SiO_2) (Refs. 9 and 10) or noble metals (Ag and Au).[14,15] Such core-shell structures are of considerable interest for many applications, which require NPs to have high magnetic susceptibility. The metallic magnetic component would provide excellent magnetic sensitivity for interaction with an external field while the passivated coating would provide a surface that could easily be functionalized.

Syntheses of the NPs through physical and chemical methods have their own advantages and disadvantages. Among various chemical synthesis methods, the borohydride reduction technique is an indispensable and versatile method, widely used for the production of NPs of FM transition metals, viz., Fe, Co, Ni, and their alloys in powdered form.[16–18] However the end product is very sensitive to reaction conditions.[16–20] Although, the resulting NPs exhibit a wide assortment of rich physical properties, may have potential applications in diverse areas, such as magnetic recording media, sensors, ferrofluids, and catalysts. However, the effectiveness of their application will depend to a large extent on their stability against oxidation and obviously on their magnetic attributes. Therefore, a thorough understanding structure and related magnetic properties of magnetic NPs prepared by the borohydride reduction method is essential if they are to have any fruitful applications. Recently, Roy *et al.*[19,20] synthesized tetragonal (t) Ni NPs by borohydride reduction method, and investigated their structural and anomalous magnetic properties. Similar temperature variation has also been reported in Ni NPs prepared through $Ni(CH_3COO)_2$ precursor and the low-temperature magnetic order has been attributed to the disorder structure of NPs.[6,7] We have extended the $Ni^{2+} \rightarrow Ni$ reaction with $NaBH_4$ in the presence of polyvinyl alcohol (PVA) in aqueous solution.

This can also throw some light on whether the interstitial oxygen enter in the lattice during chemical reduction or on exposing the particles to air after the chemical reduction.

In this paper we report a comparative study of the structure and magnetic properties of fine Ni particles with either a SSO layer and PVA coated Ni samples, prepared by the borohydride reduction method. A detailed study of magnetic properties of PVA coated and uncoated (uc-)Ni NPs indicate the presence on fcc-Ni cluster along with t-phase Ni and results in anomalous magnetic behavior at low temperature. We further delve upon the magnetic transition observed at 60 K, on which much attention has not been paid in earlier reports. Finally, a phenomenological model has been proposed that explains consistently all results obtained of the present study.

II. EXPERIMENTAL DETAILS

Fine particles of Ni were prepared by reducing the $NiCl_2 \cdot 6H_2O$ with $NaBH_4$ as reducing agent. The details of the sample preparation can be found in Ref. 19. As obtained powder sample were dried at reduced pressure (10–20 mbar) at room temperature. These samples will be referred as uc-Ni particles in our future discussion. However, for the synthesis of polymer coated (pc-)Ni particles we have carried out the chemical reduction process in the presence of PVA, i.e., Ni particles were prepared by reduction in $NiCl_2 \cdot 6H_2O$ using $NaBH_4$ in 3.0 g/dl PVA in water at room temperature. In a typical batch, a 3.0 g PVA was dissolved in 100 ml distilled water by heating at 325 K for 4 h. Subsequently, it was added dropwise to an aqueous $NiCl_2 \cdot 6H_2O$ (500 ml of 0.1 M concentration) by constant stirring at room temperature. Then, 200 ml of 1 M aqueous $NaBH_4$ was added slowly drop by drop under vigorous stirring. An exothermic reaction occurs, forming a colloidal dispersion of Ni NPs (blackish color) with the release of H_2 gas. Average temperature of the solution rises by 10–20 K. A dropwise $NaBH_4$ addition has been chosen in controlling the excess temperature. To control surface oxidation of Ni NPs, 100 ml of acetone was added to the sample before filtering and washing out NaCl and other byproduct impurities in distilled water. So as obtained powders were dried under identical conditions as stated above. Henceforth, these samples will be referred as pc-Ni particles.

The structure and microstructural characterization of the samples has been carried out using Pan-analytical X'pert PRO-PW 3040 x-ray diffractometer (using 0.15406 nm Cu $K\alpha_1$ radiation) and high-resolution transmission electron microscopic (TEM) model JEOL-JEM-2100 at an acceleration voltage 200 kV, respectively. The magnetization curves as a function of field and temperature were measured using a commercial superconducting quantum interference device magnetometer (Quantum Design). ac susceptibility (ACS) data at frequency of 80 Hz was recorded in a field of amplitude 2 Oe, using a homemade ac susceptometer.

III. EXPERIMENTAL RESULTS

A. Structure

Figure 1 compares the x-ray diffraction (XRD) patterns of the uc- and pc-Ni samples. The patterns are indicative of a

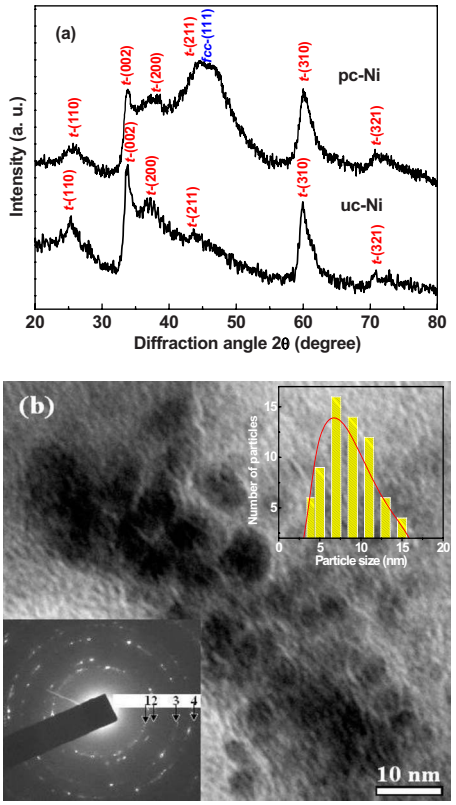

FIG. 1. (Color online) (a) X-ray diffraction pattern of uc- and pc-Ni NPs. (b) TEM image, histogram (top inset) and SAED pattern (bottom inset) of pc-Ni NPs. The labels on the SAED pattern (1) {111}, (2) {200}, (3) {220}, and (4) {311} correspond to fcc-Ni.

crystalline structure with some degree of disorder/amorphosity, which could stem from the surface layers or may be due to any defect introduced during sample preparation. All the reflections of uc-Ni shown in Fig. 1(a) are indexed assuming a t-phase with lattice parameters $a=0.4920$ nm and $c=0.5355$ nm, following an indexing scheme proposed for uc-Ni by Roy *et al.*[19,20] The XRD pattern of pc-Ni sample ($a=0.4906$ and $c=0.5332$ nm) shows a broad peak (111) at $2\theta=45°$ indicating the presence of a small fraction of fcc-Ni compared to uc-Ni. However, oxygen-stabilized t-phase of Ni dominates over the fcc phase, with (no) detectable peaks of the latter in (uc-Ni) pc-Ni XRD pattern. Peak broadenings reveal an average crystallite size ~4 nm (5 nm in the uc-Ni NPs) in the Debye-Scherrer relation. Figure 1(b) presents TEM micrograph of the pc-Ni powder. A histogram [inset of Fig. 1(b)] made with nearly 80 NPs successfully fits the log-normal distribution function, with diameters ~5–15 nm using mean diameter=7.5 nm and distribution width=0.31. The selected area electron diffractogram (SAED) shows ring pattern typical of nanocrystalline materials [inset of Fig. 1(b)]. Four distinct rings, namely (111), (200), (220), and (311) are observed in the SAED and identified as rings belonging to fcc-Ni. The XRD and SAED patterns suggest that tetragonal Ni, fcc-Ni phases coexist in pc-Ni sample. These microstructure data are further supported by the magnetic data discussed in the following section.

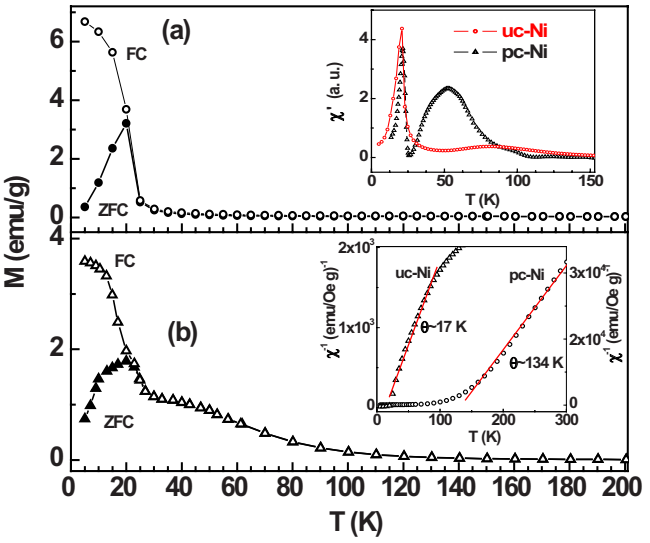

FIG. 2. (Color online) ZFC and FC plots for (a) uc- and (b) pc-Ni NPs with a magnetic field of 100 Oe. Inset (top) shows temperature dependence of the in-phase ac susceptibility (χ') and inset (bottom) shows the fit to the Curie-Weiss law.

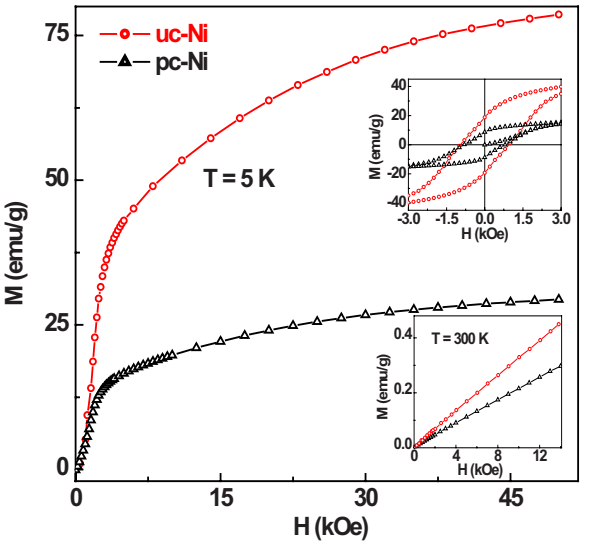

FIG. 3. (Color online) (Main panel) M-H curves measured at 5 K for uc- and pc-Ni NPs. Inset (top) shows an expanded view of the hysteresis loops over low fields and inset (bottom) M-H curves at 300 K.

B. Magnetic properties

1. Temperature-dependent dc magnetizations and ac susceptibility

Temperature dependencies of magnetization curves (M-T) were recorded in zero-field-cooling (ZFC) and field-cooling (FC) conditions under an applied field of $H=100$ Oe from 5 to 300 K, the results are shown in Fig. 2. Figure 2(a) shows the FC/ZFC curves for the uc-Ni sample for which a perfect reversibility is seen in the temperature range 25–200 K, followed by a bifurcation of ZFC/FC curves below 25 K. As the temperature is lowered below 25 K the ZFC curve shows a strong rise and finally merges with the FC curve at 20 K. This is followed by a pronounced bifurcation appears again below 20 K, with the ZFC curve forming a sharp peak at this temperature before dropping toward zero. Interestingly, FC/ZFC curves for the pc-Ni sample show reversibility in similar temperature range as uc-Ni but a steady increase in magnetization value could be seen below 250 K followed by a broad hump between 25 and 75 K [see Fig. 2(b)]. Subsequently a pronounced bifurcation again at 20 K, with the ZFC curve forming a broader peak compared to uc-Ni sample. This comparative study suggests that pc-Ni behaves differently below 150 K, where one can see some kind of magnetic ordering. The ACS measurements clearly show that pc-Ni has two distinct transitions below this temperature [see inset of Fig. 2(a)]. The origin of magnetic transition observed at 20 K seems to be similar in both samples.

2. Magnetization isotherms

The magnetic state of the uc and pc samples has been assessed through magnetization data taken at temperatures 300 and 5 K. Figure 3 shows the variation in magnetization as a function of applied field (M-H) for the pc- and uc-Ni samples at 300 K (see lower inset). Both samples have very low magnetization values and a linear magnetization response with applied field, indicative of a paramagnetic (PM) state. pc-Ni NPs show lower magnetization as nonmagnetic contribution stems from the increased nonmagnetic polymer fraction. The PM state arises of uc- and pc-Ni NPs possibly from the interstitial oxygen atoms in the t-phase.[20] Main panel of Fig. 3 shows the M-H plots at 5 K, where it is observed that the magnetization values are appreciably higher (78.5 emu/g) than the saturation magnetization of bulk fcc-Ni (58.5 emu/g at 5 K) for uc-Ni while 29.8 emu/g for pc-Ni. The M-H loops (upper inset in Fig. 3) suggest FM-like state with high coercivity (H_C) values of 954 Oe and 810 Oe for uc- and pc-Ni samples, respectively. Lower values of magnetization in pc-Ni at 5 K (consistent with the 300 K) compared to uc-Ni sample could be due to the presence of nonmagnetic polymer, though the field dependence of magnetization is essentially similar for uc- and pc-Ni samples. The enhancement in magnetization values and presence of hysteresis at 5 K compared with 300 K M-H data indicates the existence of a magnetic ordering at intermediate temperatures. However, in order to show features at 60 K transition more prominently, magnetic isotherms were recorded at various temperatures in the vicinity of peak observed in ACS curve shown in Fig. 4. As shown in the figure the uc-Ni exhibits nearly linear behavior up to high fields while pc-Ni shows the presence of two magnetic components, i.e., a sharp increase in M at low fields followed by a linear increase at higher fields. Further the M-H curves do not show H_C at these temperatures but the low-field curve resembles a superparamagnetic (SPM) natured curve. Therefore, a modified Langevin function represented by[10]

$$M(H) = M_S L\left(\frac{\mu H}{kT}\right) + \chi_f H \tag{1}$$

has been used to fit $M(H)$ data of the pc-Ni in order to quantify the magnetic parameters for the comparative study.

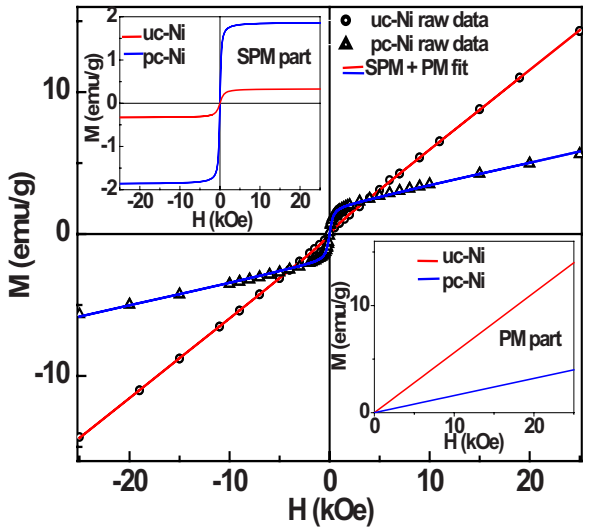

FIG. 4. (Color online) *M-H* curves for uc- (at $T=50$ K) and pc- (at $T=60$ K) Ni NPs. Solid lines through the data points represent fits to Eq. (1). Insets: (top) shows separated SPM component and (bottom) separated PM components.

Here μ is the average magnetic moment per particle $L(x)=\coth(x)-1/x$ is the Langevin function, M_S is the saturation magnetization, and χ_f is the high-field susceptibility. The solid lines through the data points in Fig. 4 are fits to Eq. (1). This quantitative analysis clearly reveals that some kind of SPM clusters develop in the case of pc-Ni with an average cluster moment $\sim 5067\ \mu_B$ at this temperature while for uc-Ni the SPM cluster moment is found to be weaker. The complete reversibility in ZFC/FC curves above 25 K along with a linear magnetization response with applied field is suggestive of a PM state of the NPs at 300 K in uc-Ni. Although pc-Ni NPs also exhibit PM state a nonlinear behavior of M in low applied magnetic fields in *M-H* curves at 300 K and the magnetic anomaly between 50 and 100 K, possibly suggest the development of magnetic clusters and blocking of a few particles containing a minority fcc phase. It is interesting to see that the intensity of 60 K peak in ACS curve appears to be more prominent in pc-Ni sample compared to uc-Ni. There are several reports that dipolar interactions between NPs can give rise to such a peak in FC magnetization.[21–23] Also for certain of the canonical spin glasses, it is reported that a small peak develops with field cooling at T_f (freezing temperature),[24] followed by a plateau below it. However, it requires further investigation and analyzed in the following discussion.

To unravel the significance of the magnetic anomalies observed at 20 and 60 K in the magnetization/ACS verses temperature curves of pc-Ni NPs, it is important to investigate magnetic isotherms taken at temperatures above and below 60 K. The magnetic isotherms spanning higher (30–300 K) and lower temperature range (5–18 K) are presented in Figs. 5(a) and 5(b), respectively. The *M-H* curves in Fig. 5(a) display low magnetization values along with rapid increase in magnetization at low magnetic fields but do not saturate even at applied fields of 50 kOe. Interestingly all the *M-H* curves above 60 K do not show H_C, yet the presence of remanence magnetization (M_r) in the intermediate temperatures suggests a FM-like behavior. This unusual *M-H* behavior could be due to the presence of two magnetic components, i.e., small FM or/and SPM clusters whose magnetization saturates at low fields and a linear component with high value of χ_f could be due to the smaller magnetic clusters or tetragonal Ni. In order to extract the parameters from the magnetic isotherms we have adopted the empirical approach having two contributions: a SPM+PM in the temperature range 60–300 K. The *M-H* isotherms have been fitted to Eq. (1) in main panel of Fig. 5(a). The fit parameters listed in Table I indicate that the cluster moment increases as the temperature is decreased to 60 K. This also implies that the spin clusters increase in size as the temperature is lowered. The χ_f value is observed to be $\sim 2.0\times10^{-5}$ emu/g Oe at 300 K, which is similar to that of uc-Ni (3.24×10^{-5} emu/g Oe). The strong PM behavior at 300 K is due to the presence of t-phase of Ni. It was suggested that the oxygen in solid solution first weakens the FM "direct exchange" between the Ni atoms and gives rise to antiferromagnetic "superexchange" interactions

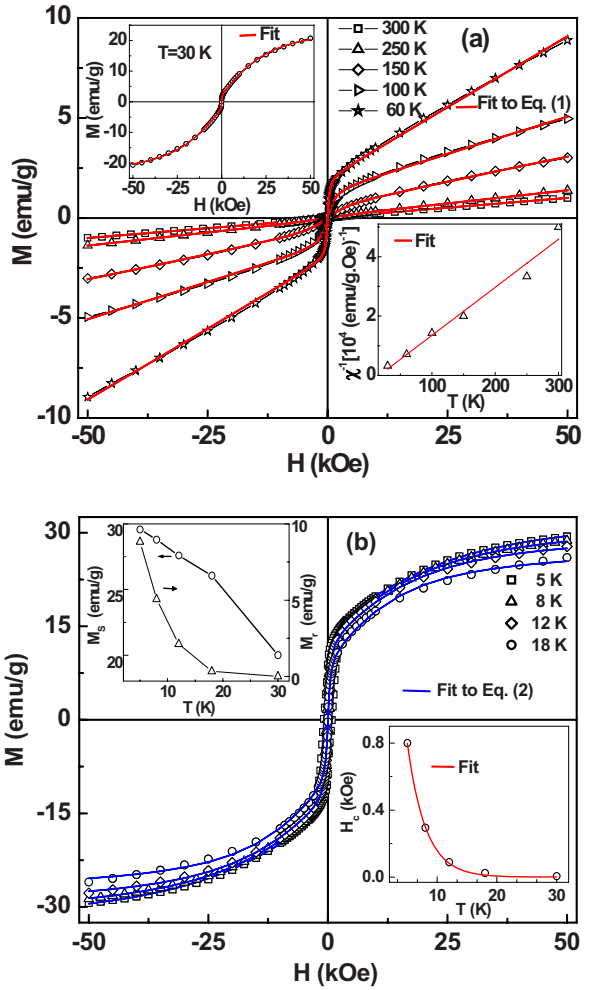

FIG. 5. (Color online) (a) *M-H* curves of pc-Ni NPs in the temperature range 60 K$\leq T\leq$300 K along with the fits to Eq. (1). Insets: (top) shows *M-H* curves at 30 K along with the fits to the two cluster model and (bottom) shows Curie-Weiss fit to the susceptibility (50 kOe). (b) *M-H* curves of pc-Ni NPs in the temperature range 5 K$\leq T\leq$30 K. Insets: (top) shows temperature dependence M_S, M_r, and (bottom) H_C as a function of temperature.

TABLE I. Parameters obtained from SPM+PM fitting Eq. (1) of *M-H* data in the temperature range 60 K$\leq T \leq$300 K for pc-Ni NPs.

Temperature (K)	M_S (emu/g)	μ (μ_B)	χ_f (emu/g Oe)
60	2.015	5067	1.4×10^{-4}
100	1.387	2426	7.0×10^{-5}
150	0.612	1347	5.0×10^{-5}
250	0.089	1326	3.0×10^{-5}
300	0.037	1304	2.0×10^{-5}

between them.[20] Subsequently the combination of these two types of interactions between the Ni atoms eliminates Ni ferromagnetism, yielding a PM state of tetragonal Ni at 300 K. Equation (1) did not yield good fits to *M-H* curves that are taken below 60 K. However, the two cluster model[10] reproduce the *M-H* data quite well at 30 K as shown in the inset (top) of Fig. 5(a) with cluster magnetic moments to be 3510 μ_B and 40 μ_B, respectively. The increase in M and χ_o observed with decreasing the temperature could be attributed to the ordering of small fcc-Ni spin cluster through exchange interactions between atomic spins. These interactions probably generate a range of magnetic clusters, where bigger clusters try to align at lower applied fields showing a sudden rise in the M while the tetragonal Ni can give rise to linear *M-H* character at higher fields with a PM behavior. It is interesting to point out here that *M-H* curves at 30 K [below the blocking temperature (T_B)] does not show significant value of H_C. This probably indicates that the clusters involved in this process are magnetically isotropic (soft) in nature and could be attributed to fcc-Ni clusters. This analysis indicates the presence of magnetic clusters in a PM matrix and enhanced intercluster interaction at lower temperatures. In the temperature range 5–30 K *M-H* data show a significant increase in M_S and M_r along with a tendency to saturate at higher applied fields. To explain such magnetic behavior one can propose three possibilities: (i) the random orientations of spins in the tetragonal Ni unit cell suggest that the large magnetization values to be intrinsic to the system or (ii) surface spins on the FM clusters can also result in nonsaturation of *M-H* curve at high fields. High magnetization values were also observed in magnetic alloy NPs prepared by the borohydride reduction method were attributed to spins at the particle surface.[11,25] De Biasi *et al.*,[11,25] observed magnetization enhancement only in diluted dispersions of their samples whereas in the present study same features are observed in totally undispersed samples (having appreciable interparticle interactions), rule out the possibility (ii). Hence the disordered spin assembly in the unit cell of oxygen-stabilized tetragonal Ni remains the only plausible reason for the magnetization enhancement at 5 K, implying the magnetization values to be intrinsic to the system. As shown in the inset (top) of Fig. 5(b), however the presence of FM behavior is evidenced by the increase in M_r and H_C below 18 K. It is clear from the *M-H* curves that below 30 K a FM character along with disappearance of linear behavior at higher applied fields is seen in the samples. Naturally the SPM+PM combination of fits fails at these temperatures. But a combination of FM+SPM contributions could be fitted to the experimental data. The *M-H* curves were fitted to the following equation comprising of FM and SPM part suggested by Stearns and Cheng:[26]

$$M(H,T) = \frac{2M_S}{\pi}\tan^{-1}\left[\frac{H \pm H_C}{H_C}\tan\left(\frac{\pi S}{2}\right)\right] + M_{SP}L\left(\frac{\mu H}{kT}\right). \tag{2}$$

The first term is the usual function customarily used to fit FM hysteresis curves while the second term accounts for the SPM component. Here "S" ($=M_r/M_S$) is known as "squareness" of the FM loop. From the analysis of the data [Fig. 5(b)] it is seen that the cluster moment increases as temperature is lowered suggesting that the cluster size grows, as the temperature is decreased. The obtained fit parameters, such as, M_S, M_r (top inset) and H_C (bottom inset) are shown in the inset [Fig. 5(b)] as a function of temperature. It is evident from the sharp increase in M_r and H_C below 18 K that magnetic ordering sets in below this temperature. The temperature dependence of H_C is fitted to an exponential law [$H_C(T)=H_{C0}\exp(-\alpha T)$] and agreement with experimental data achieved with the exponent value of 0.32 K^{-1}. Similar exponential dependence of $H_C(T)$ was reported in rare-earth transition-metal random magnets in which strong FM exchange and random magnetic anisotropy are present and the atomic moments are correlated on a small scale while magnetization rotates on a large scale through the sample. In such systems the variation in $H_C(T)$ follows an exponential behavior with temperature for different exchange and anisotropy values.[27] The exponential dependence of H_C indicates the difficulty of reversing the whole system of magnetic clusters, which change the orientation of their magnetic moments over the anisotropy energy barrier by thermal relaxation. The surface spin disorder and the dipolar interactions between the particles can give rise to large anisotropy values.

3. Spontaneous magnetization

The magnetic behavior of ferromagnetics with relatively low Curie temperature, such as, the present case has often been analyzed with the help of the so-called Arrot plots (M^2 vs H/M curves) for obtaining the spontaneous magnetic order and to establish the long-range FM order below the transition temperature. Figure 6 shows an Arrot plots of the M (H) data for $H\leq 50$ kOe. The features that are of interest in this figure can be summarized as follows. (i) The Arrot plots exhibit upward curvature for $T\leq 18$ K (without a linear component), unlike those for FM (even weak ferromagnet) materials at any given temperature. The Arrot plots are expected to result in a straight line passing through origin near T_C. (ii) No evidence of spontaneous magnetization (M_o) at any temperature (no intercept on M^2 axis). However, extrapolating from high fields produce varying intercepts, which indicates a field-induced FM alignment of the moments. (iii) A strong curvature toward the H/M axis beginning at moderate fields. (iv) At above 30 K plots exhibit downward curvature, suggesting a magnetic transition between 30 and 18 K, which is consistent with *M-T* data [see

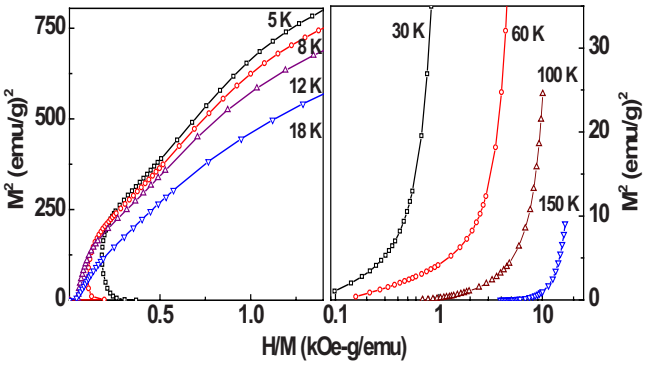

FIG. 6. (Color online) M^2 vs H/M (Arrot) plots for pc-Ni NPs in the temperature range 5 K $\leq T \leq$ 150 K.

Fig. 2(b)]. These results imply that some kind of magnetic order appear below 20 K. A strong curvature at low fields ($T \leq 18$ K) and general shape of the Arrot plot is reminiscent of the behavior theoretically predicted by Ahrony and Pytte (AP) of a random anisotropy system with weak anisotropy.[28] A transition from PM to an infinite susceptibility phase with no long-range magnetic order in zero fields has been predicted.[28] If higher order anisotropy terms are considered, the susceptibility is large but finite, i.e., the intercept on H/M axis is small but nonzero. The data in figure exhibit behavior very similar to the AP prediction that has been invoked for the interpretation of experimental results for the amorphous alloys having strong and weak anisotropy. A change in curvature in Arrot plots is not unique to amorphous FM, it also occurs in dipolar systems with random anisotropy. Another important fact is the absence of spontaneous magnetization, which implies that the FM-like behavior below 20 K is spatially confined, i.e., only clusters of FM order exist. This is in agreement with earlier conclusion that the SPM particles get blocked in a FM cluster state and also in agreement with ACS measurements on uc-Ni samples.[29] The large χ_f value ($\sim 8.7 \times 10^{-5}$ emu/g Oe) observed at 5 K in pc-Ni sample signifies the increase in the magnetization within one domain over the spontaneous value due to redistribution in the populations of spins at high fields.

4. Magnetic anisotropy

We have attempted to estimate the effective anisotropy constant (K_{eff}) by fitting the magnetization data (M-H curve at 5 K) in the approach to saturation regime, which can be expressed as[30]

$$M = M_o\left(1 - \frac{4K_{eff}^2}{15M_0^2H^2}\right) + \chi_f H. \tag{3}$$

Excellent fit was obtained for 5 K M-H data with Eq. (3) in the field range 20 kOe $< H <$ 50 kOe and the values of M_o, χ_f, and K_{eff} are 25.62 emu/g, 0.87×10^{-4} emu/g Oe, and 3.62×10^5 erg/cm^3, respectively. The K_{eff} of bulk Ni is 8×10^5 erg/cm^3 that is of similar order as obtained in present case. Relatively high level of anisotropy that seems to characterize this system suggests that in the low-temperature state the anisotropy is stronger. More likely situation is that there are FM correlated regions, the sizes of which are limited by the grain sizes, whose magnetization directions are pinned or frozen by random anisotropy. We have attempted to estimate the magnetic cluster size from the experimentally obtained T_B and K_{eff} values. The size or volume of the cluster can be determined through $V = 25kT_B/K_{eff}$ (k is the Boltzmann constant). The average magnetic particle size is obtained to be 10 nm, which is in agreement with the structural data.

IV. DISCUSSION

A comparative structural analysis of both pc- and uc-Ni suggest that NPs shows tetragonal Ni structure but pc-Ni shows a small fraction of fcc-Ni though the samples were prepared under identical conditions. The presence of minute fcc-Ni phase in pc-Ni suggests that due to the presence of PVA it is possible that the penetration of oxygen into the fcc crystal lattice is curtailed, which results in the formation of few fcc-Ni sites rather than tetragonal Ni. Evidence for the fcc-Ni in the NPs comes from SAED patterns taken on the pc-Ni sample, which is further confirmed through the magnetic measurements.

At 300 K uc-Ni shows PM behavior (linear M-H plot at low and high magnetic fields) due to the tetragonal Ni, where each particle having a PM collection of atomic spins within it and hence no magnetic moment.[20] Although pc-Ni also exhibits similar features at high applied field but a nonlinear variation in M-H plot is discernible at low field. Indeed the Langevin-type M-H variation at low fields suggests the presence of SPM clusters. To further verify the existence of SPM state in a material one needs to satisfy the two basic requirements, namely (i) the M-H curve must not show hysteresis since that is not a thermal equilibrium property and (ii) the M-H curve for an isotropic sample must be temperature dependent to the extent that curves taken at different temperature must approximately superimpose when plotted against H/T after correction for the temperature dependence of the spontaneous magnetization value. All the normalized isotherms obtained from the two component fits [Eq. (1)] in the temperature range 60 K $\leq T \leq$ 300 K are plotted against H/T in Fig. 7(a). It can be seen that the M-H curves $T \geq 150$ K superpose one on other while deviations have been observed for the $T \leq 100$ K. These observations suggest that pc-Ni NPs are magnetically heterogeneous possibly with core-shell geometry. It can be speculated that the SPM behavior down to 150 K is due to the presence of tiny cluster of fcc-Ni present in tetragonal Ni particle. Such a magnetic behavior is quite common in metallic magnetic clusters which imply that the inner layer atoms have bulk magnetic moment but atoms near the surface did not.[31] Similarly, it was also claimed for platinum clusters that the inner-core displayed "metallic" character like that of bulk whereas the surface did not.[32] As discussed in the introduction, a generalization of core-shell structure for metallic NPs is not unreasonable given the oxidation effects and broken symmetry at the surface. For the temperature range 60 K $\leq T \leq$ 100 K the normalized initial M-H curve do not overlap, which could be interpreted in the following two ways: (i) increase in the

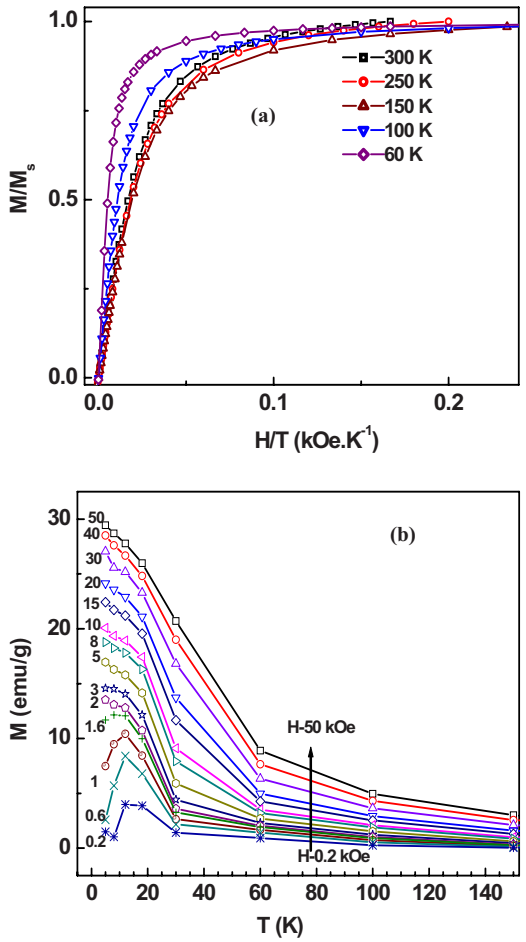

FIG. 7. (Color online) (a) M/M_S vs H/T plots of SPM part for pc-Ni NPs in the temperature range 60 K $\leq T \leq$ 300 K. (b) M vs T plots for pc-Ni NPs obtained from the M-H curves at different fields.

magnetization below 100 K could be due to reduction in thermal fluctuation of spin moments around the core clusters (fcc-Ni) and (ii) the enhancement in the intercluster interaction strength, which eventually freeze in random fashion at 60 K. A significant increase in magnetization below 60 K and a tendency of saturation in M-H curves at 30 K in high fields suggests that the tiny fcc-Ni clusters contribute to net increase in magnetization.

Coming to the low-temperature magnetic state of both uc- and pc-Ni samples, it can be said that the bifurcation in the FC/ZFC curves of these samples at ~20 K is a typical signature of the metastable nature of the magnetization and is exhibited by various magnetically disordered systems, such as, spin glasses, cluster glasses, superparamagnets, and even inhomogeneous ferromagnets. In fact in case of single-domain fine particles, the maximum in the ZFC curve is roughly defined as T_B. T_B is very much sensitive to the strength of interparticle dipolar interactions. This interaction strength depends on SPM particle concentration and distance between them, which in the present study is in turn dependent on the molar concentration of the $NiCl_2$ solution from which the NPs have been prepared and also should have significant effect on T_B when PVA matrix is present. But no such change in the transition temperature of ~20 K was observed when the M-T curves were repeated for samples prepared from $NiCl_2$ solution of different molar concentrations.[33] This rules out the possibility of 20 K being a T_B of SPM particles. The appearance of a maximum at 20 K in the ZFC and ACS curves of uc- and pc-Ni samples therefore suggests that the transition at 20 K is intrinsic to the system. It is independent of external parameters, such as, sample molarity and the presence/absence of PVA coating and may therefore owe its origin to the modified structure of the Ni lattice, i.e., tetragonal Ni. This is quite logical since the peak at 20 K is present in the ZFC curve of only as-prepared samples and not for annealed samples, which do not constitute t-phase Ni.[34]

We attribute the peak at 20 K to a PM-FM-like phase transition involving the internal ordering of the spins inside each particle, whereby the hitherto PM t-phase Ni inside a particle becomes FM ordered.[20] The reciprocal susceptibility $(1/\chi)$ plotted as a function of T [inset (bottom) of Fig. 5(a)] could be fitted to the Curie-Weiss law $[\chi = C/(T-\theta)]$ for $T > T_{max}$ with an ordering temperature θ of $\sim 17 \pm 3$ K, suggesting the onset of strong magnetic interactions and therefore corroborating our proposition. This FM ordering inside a particle imparts large magnetic moment to the particle. However, as shown in Fig. 7(b) the sharp peak observed in ZFC curve gets suppressed on application of a 3 kOe field at 5 K. Subsequent raise in magnetization at higher fields suggest that the spin moments are rotated from their frozen directions and then aligned in the direction of the applied field, thereby leading to the large magnetization enhancement observed at this temperature. It is interesting to point out here that the presence of a PM component in the M-H plots at 300 K and the peak at 20 K in ZFC curves appear in both pc- and uc-Ni samples. We therefore believe that it is the t-phase of Ni which gives rise to the above features (PM component and peak at 20 K) because of the disordered collection of spins in the unit cell.

In order to explain the surprising features of the XRD patterns and M-H curves of pc-Ni sample more coherently, a phenomenological model based on the results obtained though detailed analysis of the above data is presented in Fig. 8. Figure 8(a) shows a particle of the pc sample is an interstitial solid solution of Ni and oxygen while the core contains fcc-Ni and the entire particle is encapsulated in PVA outer layer. Here the dissolved oxygen atoms play the central role in drastically reducing the magnetization by giving rise to a certain degree of frustration of the Ni moments. This, coupled with the random orientation of the spins of Ni atoms in a particle, causes the net magnetic moment of each particle to be quite small. Therefore SPM relaxation of particle moment occurs and the ensemble of particles acts as a PM with completely unordered and unrelated individual moments. When the temperature is reduced below 70 K as shown in Fig. 8(b) the small core Ni clusters (behave like SPM above 150 K) get blocked in random direction, which results in increase in magnetization. At lower temperatures the magnetic behavior of tetragonal Ni dominates over the fcc-Ni. Figure 8(c) represents that individual particle moments are aligned in random directions and freeze below 20 K in random fashion that is similar to a cluster glass. On

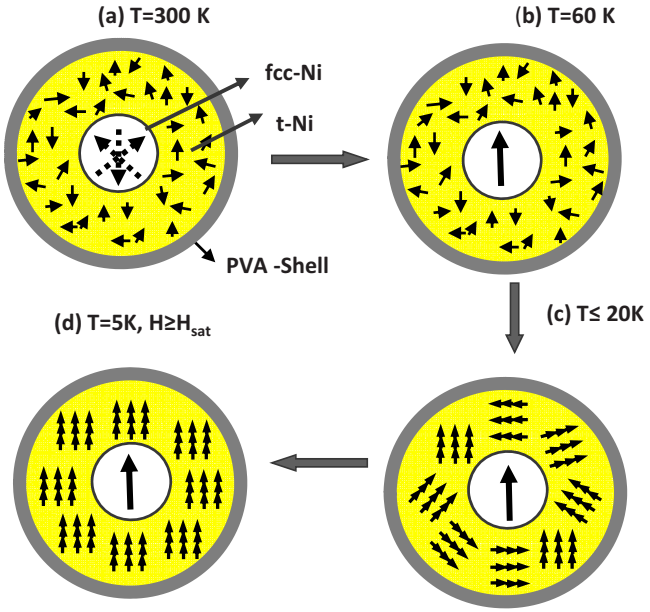

FIG. 8. (Color online) A phenomenological model of magnetic contributions in the pc-Ni NPs.

application of magnetic field at 5 K, the macromoments or superspins rotate (including fcc-Ni core moments) from their frozen directions and then align in the direction of the applied field, leading to the large magnetization enhancement observed in the *M-H* plot at this temperature [Fig. 8(d)]. However, the complete saturation of *M-H* curves is not observed experimentally which could be due to shape anisotropy of the particles. Finally it should be pointed out here that autocombustion pc-Ni develops into a carbon coated nanotubules, which present an excellent magnetic properties with high stability and can be strong candidates for technological applications.[34]

V. CONCLUSION

A comparative study of structure and magnetic properties of pc- and uc-Ni NPs has been carried out. From these investigations it can be concluded that (i) in the pc-Ni sample the PVA shell prevents the formation of the SSO layer. This is much desired since the properties exhibited by the sample would now be that due to its free-standing transition-metal NPs. This also results in the development of small fcc-Ni cluster during synthesis. The pc-Ni particles are much smaller (~7 nm) in size compared to uc samples.

(ii) The crystal structure (tetragonal) arising from the incorporation of oxygen atoms in the unit cell of fcc-Ni gives rise to anomalous magnetic behavior, such as a huge magnetization enhancement at low temperatures for both pc- and uc-Ni samples.

(iii) The FC/ZFC and ACS plots reveal the occurrence of two magnetic transitions at 60 and 20 K in the pc-Ni sample and only the former transition in the sample has the features that are reminiscent of cluster freezing/blocking and attributed to small fcc-Ni core while the low-temperature transition is entirely due to the structure and composition of the oxygen-stabilized tetragonal Ni NPs.

(iv) The features observed at 20 K in the ACS and *M-T* plots have been related to a PM to FM-like phase transition though there is no evidence of a long-range FM order. This can also be attributed to the cooperative freezing of FM clusters.

(v) Finally, a phenomenological model has been proposed that explains consistently all results obtained in the present study.

ACKNOWLEDGMENTS

The authors thank A. Roy, S. Ram (IIT, Kharagpur) and J. A. De Toro (Universidad de Castilla—La Mancha, Spain) for the helpful discussions. This work was supported by Armament Research Board, DRDO, New Delhi, India. One of the authors (V. Singh) gratefully acknowledges the CSIR, Government of India, for support. Work at Seoul National University was supported by the National Research Foundation of Korea.

*Corresponding author. FAX: +91-3222-255303; veeturi@phy.iitkgp.ernet.in

†Present address: Centre for Liquid Crystal Research, Bangalore–560 013, India.

‡Present address: Department of Physics and Astronomy, Center for Strongly Correlated Materials Research, Seoul National University, Seoul 151-742, Korea.

[1] S. Bedanta and W. Kleemann, J. Phys. D **42**, 013001 (2009); E. Winkler, R. D. Zysler, M. V. Mansilla, D. Fiorani, D. Rinaldi, M. Vasilakaki, and K. N. Trohidou, Nanotechnology **19**, 185702 (2008).

[2] L. Del Bianco, F. Boscherini, A. L. Fiorini, M. Tamisari, F. Spizzo, M. V. Antisari, and E. Piscopiello, Phys. Rev. B **77**, 094408 (2008).

[3] In Su Lee, N. Lee, J. Park, B. H. Kim, Y. W. Yi, T. Kim, T. K. Kim, I. H. Lee, S. R. Paik, and T. Hyeon, J. Am. Chem. Soc. **128**, 10658 (2006); J. Park, E. Kang, S. U. Son, H. M. Park, M. K. Lee, J. Kim, K. W. Kim, H. J. Noh, J. H. Park, C. J. Bae, J. G. Park, and T. Hyeon, Adv. Mater. **17**, 429 (2005).

[4] K. Sakiyama, K. Koga, T. Seto, M. Hirasawa, and T. Orii, J. Phys. Chem. B **108**, 523 (2004).

[5] V. Tzitzios, G. Basina, M. Gjoka, V. Alexandrakis, V. Georgakilas, D. Niarchos, N. Boukos, and D. Petridis, Nanotechnology **17**, 3750 (2006).

[6] W. C. Nunes, E. De Biasi, C. T. Meneses, M. Knobel, H. Winnischofer, T. C. R. Rocha, and D. Zanchet, Appl. Phys. Lett. **92**, 183113 (2008).

[7] E. De Biasi, A. Leon-Vanegas, W. C. Nunes, S. k. Sharma, P. Haddad, T. C. R. Rocha, J. G. S. Duque, D. Zanchet, and M. Knobel, Eur. Phys. J. B **66**, 503 (2008).

[8] L. Del Bianco, D. Fiorani, A. M. Testa, E. Bonetti, L. Savini, and S. Signoretti, J. Magn. Magn. Mater. **262**, 128 (2003).

[9] J. C. Denardin, A. L. Brandl, M. Knobel, P. Panissod, A. B. Pakhomov, H. Liu, and X. X. Zhang, Phys. Rev. B **65**, 064422 (2002).
[10] X. Chen, S. Bedanta, O. Petracic, W. Kleemann, S. Sahoo, S. Cardoso, and P. P. Freitas, Phys. Rev. B **72**, 214436 (2005).
[11] E. De Biasi, C. A. Ramos, R. D. Zysler, and H. Romero, Phys. Rev. B **65**, 144416 (2002).
[12] H. Kisker, T. Gessmann, R. Wurschum, H. Kronmuller, and H. E. Schaefer, Nanostruct. Mater. **6**, 925 (1995).
[13] L. Del Bianco, A. Hernando, M. Multigner, C. Prados, J. C. Sanchez-Lopez, A. Fernandez, C. F. Conde, and A. Conde, J. Appl. Phys. **84**, 2189 (1998).
[14] E. E. Carpenter, J. A. Sims, J. A. Wienmann, W. L. Zhou, and C. J. O'Connor, J. Appl. Phys. **87**, 5615 (2000).
[15] T. Bala, S. K. Arumugum, R. Pasricha, B. L. V. Prasad, and M. Sastry, J. Mater. Chem. **14**, 1057 (2004); D. S. Sidhaye, T. Bala, S. Srinath, H. Srikanth, P. Poddar, M. Sastry, and B. L. V. Prasad, J. Phys. Chem. C **113**, 3426 (2009).
[16] G. N. Glavee, K. J. Klabunde, C. M. Sorensen, and G. C. Hadjipanayis, Langmuir **10**, 4726 (1994).
[17] J. Legrand, A. Taleb, S. Gota, M. J. Guittet, and C. Petit, Langmuir **18**, 4131 (2002).
[18] J. P. Chen, C. M. Sorensen, K. J. Klabunde, and G. C. Hadjipanayis, Phys. Rev. B **51**, 11527 (1995).
[19] A. Roy, V. Srinivas, S. Ram, J. A. De Toro, and J. M. Riveiro, J. Appl. Phys. **96**, 6782 (2004).
[20] A. Roy, V. Srinivas, S. Ram, J. A. De Toro, and U. Mizutani, Phys. Rev. B **71**, 184443 (2005).
[21] R. W. Chantrell, N. S. Walmsley, J. Gore, and M. Maylin, J. Magn. Magn. Mater. **196-197**, 118 (1999).
[22] R. D. Zysler, D. Fiorani, and A. M. Testa, J. Magn. Magn. Mater. **224**, 5 (2001).
[23] J. M. Vargas, W. C. Nunes, L. M. Socolovsky, M. Knobel, and D. Zanchet, Phys. Rev. B **72**, 184428 (2005).
[24] J. A. Mydosh, *Spin Glasses: An Experimental Introduction* (Taylor & Francis, London, 1993).
[25] R. D. Zysler, H. Romero, C. A. Ramos, E. De Biasi, and D. Fiorani, J. Magn. Magn. Mater. **266**, 233 (2003).
[26] M. B. Stearns and Y. Cheng, J. Appl. Phys. **75**, 6894 (1994).
[27] R. Ribas, B. Dieny, B. Barbara, and A. Labarta, J. Phys.: Condens. Matter **7**, 3301 (1995).
[28] A. Aharony and E. Pytte, Phys. Rev. Lett. **45**, 1583 (1980).
[29] A. Roy, V. Srinivas, J. A. De Toro, and J. P. Goff, Phys. Rev. B **74**, 104402 (2006).
[30] E. M. Chudnovsky, W. M. Saslow, and R. A. Serota, Phys. Rev. B **33**, 251 (1986); G. Hadjipanayis, D. J. Sellmyer, and B. Brandt, *ibid.* **23**, 3349 (1981).
[31] M. L. Billas, A. Chatelain, and W. A. de Herr, Science **265**, 1682 (1994).
[32] F. M. Mulder, T. A. Stegink, R. C. Thiel, L. J. de Jongh, and G. Schmid, Nature (London) **367**, 716 (1994).
[33] A. Roy, Ph.D. thesis, Indian Institute of Technology Kharagpur, 2006.
[34] V. Singh, S. Ram, M. Ranot, J. G. Park, and V. Srinivas, Appl. Phys. Lett. **92**, 253104 (2008).